ELECTROMAGNETIC LOWER HYBRID INSTABILITY IN THE SOLAR WIND

G. S. LAKHINA

Indian Institute of Geomagnetism, Colaba, Bombay, India

(Received 8 October, 1984)

Abstract. Low frequency electromagnetic lower hybrid waves (so-called hybrid whistlers) propagating nearly transverse to the magnetic field can be driven unstable by a resonant interaction with 'halo' electron distributions carrying solar wind heat flux. The electromagnetic lower hybrid instability is excited when the 'halo' electron drift exceeds the parallel phase velocity of the wave. The growth rate attains a maxima at a certain value of the wavenumber. The maximum growth rate decrease by an increase in $\beta_{\perp e}$ (the ratio of electron pressure to magnetic field pressure) and 'halo' electron temperature anisotropy. At 0.3 AU the growth time of the electromagnetic lower hybrid instability is of the order of 25 ms or shorter, whereas the most unstable wavelengths associated with the instability fall typically in a range of 27 to 90 km. The instability would give rise to a local heating of solar wind ions and electrons in the perpendicular and parallel directions relative to the magnetic field, $\mathbf{B}_0$. The observations of low frequency whistlers having high values of B/E ratios (B and E being the magnitude of the wave magnetic and electric field, respectively) and propagating at large oblique angles to $\mathbf{B}_0$ behind interplanetary shocks, can be satisfactorily explained in terms of electromagnetic lower hybrid instability. The instability is also relevant to the generation mechanism of correlated whistler and electron plasma oscillation bursts detected on ISEE-3.

1. Introduction

Data from ISEE-3 and Helios spacecrafts indicate the presence of low frequency ($\omega \ll \Omega_e$, ω and Ω_e being, respectively, the wave frequency and the electron cyclotron frequency) waves propagating at large angles to the interplanetary magnetic field, $\mathbf{B}_0$, in the solar wind plasma (Coroniti *et al.*, 1982; Kennel *et al.*, 1982; Beinroth and Neubauer, 1981). Such a low frequency turbulence often exhibits broadband electrostatic noise accompanied by bursts of electromagnetic noise (Gurnett and Frank, 1978; Scarf *et al.*, 1981). The electrostatic noise is usually identified as ion acoustic waves (Gurnett *et al.*, 1979). Since most of the time conditions for the excitation of ion acoustic waves are not satisfied in the solar wind (Dum *et al.*, 1981) an alternative explanation for the electrostatic noise in terms of lower hybrid waves has been proposed by Marsch and Chang (1982).

The low fequency electromagnetic noise in the disturbed solar wind has been identified as whistler mode propagating very obliquely to $\mathbf{B}_0$ by Coroniti *et al.* (1982). Marsch and Chang (1983) have suggested that the low frequency electromagnetic noise can be generated by an electromagnetic lower hybrid instability driven by the resonant 'halo' electron component. Marsch and Chang (1983) have solved numerically the dispersion relation for obliquely propagating low frequency waves in the range $\Omega_i \ll \omega \ll \Omega_e$. In their work thermal effects are retained as corrections for the electron electromagnetic terms but are neglected altogether for ions. Their analysis is, therefore, valid for vanishingly small values of $\beta_e = (8\pi n_0 K_B T_e/B_0^2)$ and $\lambda_e = (k_\perp^2 \alpha_{\perp e}^2/2\Omega_e^2)$,

Astrophysics and Space Science **111** (1985) 325–334. 0004–640X/85.15

$\alpha_{\perp e} = (2K_B T_e/m_e)^{1/2}$ being the thermal velocity of electrons. Marsch and Chang (1983) find that inclusion of electromagnetic effects (i.e. considering $\omega_{pe}/ck \neq 0$) reduces the growth rate of the lower hybrid waves as compared to the purely electrostatic case (i.e., $\omega_{pe}/ck = 0$).

Non-resonant lower hybrid instabilities driven by solar wind electron heat flux has been investigated earlier by Lakhina (1979, 1981). The non-resonant instability is distinguished from the resonant instability by the fact that the former arises from the real part of the dispersion relation only, whereas the latter requires a finite imaginary part of the dispersion function (i.e. Im $D \neq 0$ is a must). The threshold for excitation of the non-resonant lower hybrid instability under a fully electromagnetic treatment was found to be one order higher than the electrostatic case (Lakhina, 1979). For average solar wind conditions at 1 AU, excitation of non-resonant electromagnetic lower hybrid instability requires core electron drift speeds larger than $8v_A$ (v_A being the Alfvén speed).

In this paper we study analytically a fully electromagnetic lower hybrid instability of resonant type as discussed by Marsch and Chang (1983). We generalized the analysis of Marsch and Chang (1983) for arbitrary values of $\beta_{\perp C}$ and λ_C (subscript 'C' denotes core electrons) (Section 2). We fnd that the growth rate of the electromagnetic lower hybrid instability peaks at a certain value of λ_C (say λ_m). An increase in $\beta_{\perp C}$ reduces the growth rate. At 0.3 AU the typical growth time for the instability is found to be of the order of 25 ms or less. It is shown that for $U_H \lesssim \alpha_{\parallel H}$ (U_H and $\alpha_{\parallel H}$ being the drift speed and the thermal speed of the 'halo' electrons, respectively), the lower hybrid instability can have significant growth rate whereas the high frequency plasma oscillations are damped (Section 3). For $U_H > \alpha_{\parallel H}$, both the lower hybrid and electron plasma oscillations are excited thereby explaining the observations of occasional correlated whistler and plasma oscillation bursts in the disturbed solar wind (Kennel *et al.*, 1980). Relevance of electromagnetic lower hybrid instability to the obliquely propagating whistler, characterised by large values of refractive indices, detected behind interplanetary shocks in the solar wind is also discussed in Section 3.

2. Dispersion Relation

Let us model the solar wind core and halo electrons as two Maxwellians with a relative drift. In the frame of reference moving with bulk speed of the solar wind, protons do not possess any drift and can be described by a Maxwellian distribution function with temperature T_p. The 'core' and 'halo' electron will then be streaming along the interplanetary magnetic field $\mathbf{B}_0 = B_0 \hat{e}_z$ with velocities $\mathbf{U}_C = -U_C \hat{e}_z$ and $\mathbf{U}_H = U_H \hat{e}_z$, respectively. The subscripts C and H refer to 'core' and 'halo' electrons, respectively. The observations show that within experimental error, the conditions

$$N_p = N_C + N_H ,$$

and

$$N_C U_C + N_H U_H = 0 , \tag{1}$$

are satisfied (Feldman *et al.*, 1975; Bame *et al.*, 1975; Marsch *et al.*, 1982). We make the following assumptions to derive the dispersion relation for the electromagnetic lower hybrid waves:

(1) We consider the frequency range $\Omega_p^2 \ll |\omega|^2 \ll \Omega_e^2$ where ω, Ω_p, and Ω_e are the wave frequency, proton cyclotron frequency, and electron cyclotron frequency, respectively, with $\gamma > \Omega_p$ (γ being the growth rate). This allows us to treat the protons as essentially unmagnetised.

(2) We consider nearly transverse propagating waves with $k_\parallel \ll k_\perp$ where $k_\parallel$ and $k_\perp$ are wavenumbers parallel and perpendicular to $\mathbf{B}_0$, respectively.

(3) We consider the case $\omega^2 \gg k_\perp^2 \alpha_p^2$ and $(\omega - \mathbf{k}\cdot\mathbf{U}_C)^2 \gg k_\parallel^2 \alpha_{\parallel C}^2$; where the Landau damping due to protons as well as core electrons can be neglected.

(4) We consider $(\omega - \mathbf{k}\cdot\mathbf{U}_H)^2/k_\parallel^2 \alpha_{\parallel H}^2 \ll 1$, so that the halo electrons can interact resonantly with the waves and excite the instability.

(5) Furthermore, we consider that $|\mathbf{k}\cdot\mathbf{U}_C|^2 \ll |\omega^2| \lesssim |\mathbf{k}\cdot\mathbf{U}_H|^2$, which simply means that the parallel phase velocities are much larger than the core drift speed but are of the same order as the halo electron drift speed.

Then, the fully electromagnetic dispersion relation as given by Equation (2) of Lakhina (1979) or Equation (1) of Marsch and Chang (1983) simplifies to:

$$D = \mathrm{Re}D + i\,\mathrm{Im}D = 0\,, \tag{2}$$

where the real and the imaginary parts of D are given by

$$\mathrm{Re}D = p\omega^4 + q\omega^2 + r\,, \tag{3}$$

$$\mathrm{Im}D = -\left[2\sqrt{\pi}\,\frac{\omega_{pH}^2(\omega - k_\parallel U_H)}{k_\parallel \alpha_{\parallel H}}\right](S_1 + S_2 - S_3)\,, \tag{4}$$

$$p = a(1+a)\alpha + 8\omega_{pC}^6 U_C^2 \phi_C^3 v^2/k_\perp^4 \alpha_{\perp C}^6\,, \tag{5}$$

$$\begin{aligned} q = {} & -\alpha[b(1+2a) + (1+a)c^2k^2(1+\beta_{\perp C}\psi_C) + \omega_{pC}^4\psi_C^2/\Omega_e^2] - \\ & - ac^2k_\parallel^2\omega_{pC}^2(1 - \phi_C - R\phi_C) - \omega_{pC}^2\phi_C \times \\ & \times \left\{2aRc^2k_\parallel^2(1 - aR\alpha_{\perp C}^2/4c^2) + \frac{2aU_C^2v^2}{\alpha_{\perp C}^2} \times \right. \\ & \left. \times \left[b + c^2k^2(1+\beta_{\perp C}\psi_C) + \frac{2\omega_{pC}^2\psi_C^2\lambda_C\sigma}{\phi_C v}\right]\right\} + \\ & + \beta_{\perp C}\omega_{pC}^2c^2k^2U_C^2\psi_C^2\sigma^2/\alpha_{\perp C}^2\,, \end{aligned} \tag{6}$$

$$\begin{aligned} r = {} & b\alpha[b + c^2k^2(1+\beta_{\perp C}\psi_C)] + c^2k_\parallel^2\{[\omega_{pC}^2(1 - \phi_C - R\phi_C) + \\ & + 2R(1 - \omega_{pC}^2R\phi_C/2c^2k_\perp^2)\omega_{pC}^2\phi_C][b + c^2k^2(1+\beta_{\perp C}\psi_C)] - \\ & - \beta_{\parallel C}\omega_{pC}^2k_\perp^2c^2\psi_C^2 + \beta_{\parallel C}\psi_C^2\omega_{pC}^4R\phi_C\} + \\ & + c^2k^2\beta_{\parallel C}\omega_{pC}^2[(1+a)k_\parallel^2\alpha_{\parallel C}^2/4 - bU_C^2\sigma^2/\alpha_{\parallel C}^2]\,, \end{aligned} \tag{7}$$

$$S_1 = \frac{\omega^2(1-\phi_H)}{k_\parallel^2 \alpha_{\parallel H}^2} \{\omega^2[(1+a)a\omega^2 - b(1+2a) - c^2k^2(1+a)(1+\beta_{\perp C}\psi_C) - \omega_{pC}^4\psi_C^2/\Omega_e^2] + (b + c^2k_\parallel^2)[b + c^2k^2(1+\beta_{\perp C}\psi_C)]\}, \tag{8}$$

$$S_2 = \frac{c^2k^2\beta_{\perp C}\psi_H T_{\perp H}^2}{T_{\parallel H}T_{\perp C}} \left\{(-\omega^2 + b)(1 - \phi_C - R\phi_C + c^2k^2/\omega_{pC}^2) + c^2k_\parallel^2[1 - \phi_C + R\phi_C(1 - \omega_{pC}^2 R\phi_C/c^2k_\perp^2)] - 2a\omega^2\left[\frac{U_C^2\phi_C v^2}{\alpha_{\perp C}^2} + \frac{c^2k^2}{\omega_{pC}^2}\frac{k_\parallel U_C v}{\omega}\left(1 - \frac{\omega_{pC}^2 R\phi_C}{c^2k_\perp^2}\right)\right]\right\}, \tag{9}$$

$$S_3 = c^2k^2\omega^2\beta_{\perp C}\psi_H\psi_C\left[\frac{c^2}{\alpha_{\perp C}^2} + \frac{U_C\omega}{k_\parallel \alpha_{\perp C}^2}(1 + 2a + b/\omega^2) + \frac{1}{2}\left(\frac{b}{\omega^2}\frac{T_{\parallel C}}{T_{\perp C}} - a\right)\right], \tag{10}$$

$$R = \left[T_{\parallel C}/T_{\perp C} - 1 + \frac{2U_C^2}{\alpha_{\perp C}^2}\left(1 + \frac{N_C\phi_H T_{\perp C}}{N_H\phi_C T_{\perp H}}\right)\right], \tag{11}$$

$$a = 2\omega_{pC}^2\phi_C/k_\perp^2\alpha_{\perp C}^2;$$

$$b = (\omega_{pP}^2 - k_\parallel^2\omega_{pC}^2 R\phi_C/k_\perp^2), \tag{12}$$

$$\alpha = [\omega_{pC}^2 + c^2k^2 - \omega_{pC}^2\phi_C(1+R)], \tag{13}$$

$$\sigma = (1 - \psi_H/\psi_C);$$

$$v = (1 - \phi_H T_{\perp C}/\phi_C T_{\perp H}),$$

$$\psi_j = [I_0(\lambda_j) - I_1(\lambda_j)]\, e^{-\lambda_j},$$

$$\phi_j = [1 - I_0(\lambda_j)\, e^{-\lambda_j}], \tag{14}$$

where $I_0(\lambda_j)$ and $I_1(\lambda_j)$ are, respectively, the modified Bessel functions of order 0 and 1 with the argument $\lambda_j = (k_\perp^2\alpha_{\perp j}^2/2\Omega_j^2)$ and $j = C$ for core electrons and H for halo electrons. The subscript $\parallel$ and $\perp$ denote the quantities parallel and perpendicular to the magnetic field, respectively.

Equation (2) is solved by writing $\omega = \omega_r + i\gamma$ and assuming that $|\gamma^2| \ll |\omega_r^2|$, where $\gamma > 0$ denotes instability. The real frequency ω_r can then be obtained from $\mathrm{Re}\, D = 0$, which gives

$$\omega_r = [-q \pm (q^2 - 4pr)^{1/2}]/2. \tag{15}$$

The growth rate is given by the relation

$$\gamma = -\operatorname{Im} D \Big/ \frac{\partial \operatorname{Re} D}{\partial \omega_r} = -\operatorname{Im} D / 2\omega_r (2p\omega_r^2 + q) . \tag{16}$$

The above expressions for ω_r and γ are valid for arbitrary values of $\beta_{\perp C}$ as well λ_C.

On taking the limit $\omega_{pC}^2/c^2k^2 \to 0$ in Equations (15) and (16) we get electrostatic lower hybrid waves with

$$\omega_r = \frac{[\omega_{pP}^2 + k_\parallel^2 \omega_{pC}^2 (1 - \phi_C)/k_\perp^2]^{1/2}}{(1 + 2\omega_{pC}^2 \phi_C / k_\perp^2 \alpha_{\perp C}^2)^{1/2}} \tag{17}$$

and

$$\gamma = \frac{2\sqrt{\pi} N_H}{N_C} \frac{\omega_{pC}^2 \omega_r}{k_\perp^2 k_\parallel \alpha_{\parallel H}^3} \frac{(k_\parallel U_H - \omega_r)}{(1 + 2\omega_{pC}^2 \phi_C / k_\perp^2 \alpha_{\perp C}^2)} . \tag{18}$$

It is clear that γ will be positive only when $U_H > \omega_r/k_\parallel$, and it increases with the increase of N_H/N_C, $k_\parallel$, and U_H and a decrease of $\alpha_{\parallel H}$.

In the limit of $m_i/m_e \gg \omega_{pC}^2/c^2k^2 \gg 1$, which allows us to treat the electrons' response as electromagnetic and that of protons as electrostatic, and for vanishingly small $\beta_{\perp C}$, Equations (15) and (16) yield simple expressions for electromagnetic lower hybrid waves:

$$\omega_r = \frac{\omega_{pP}}{\omega_{pC}} \Omega_e \left(\frac{ck}{\omega_{pC}} \right) (1 + \beta_{\perp C}/2) , \tag{19}$$

$$\gamma = \sqrt{\pi} \frac{\omega_r N_H^2}{N_C^2} \frac{(k_\parallel U_H - \omega_r)}{k_\parallel \alpha_{\parallel H}} \left(\frac{U_H}{c} \frac{k_\perp}{k_\parallel} \frac{\omega_{pP}}{\Omega_e} \right) (1 - \beta_{\perp C}/2) . \tag{20}$$

Equation (20) shows that the instability would occur when U_H exceeds the parallel phase velocity of the wave. Since ω_r is proportional to (ck/ω_{pC}), the real frequency as well as γ would decrease with the increase of the parameter (ω_{pC}/ck), which measure the extent of electromagnetic nature of the wave. From Equations (19) and (20), it is clear that the inclusion of $\beta_{\perp C}$ has a stabilizing effect, although small.

For arbitrary values of λ_C and $\beta_{\perp C}$, the real frequency ω_r and growth rate γ can be evaluated numerically directly from Equations (15)–(16). Some numerical results are shown in Figures 1 to 3.

From Figure 1, it is clear that the growth rates increase, attain a maxima and then decrease as λ_C is increased from small to large values (cf. solid curves). The real frequency ω_r, increases and then saturates as λ_C increases (cf. dashed curve 1). Further, the curves 1 to 4 indicate that for a fixed value of U_C, there exists an optimum value of density ratio N_H/N_C where the growth rates are maximized with respect to N_H/N_C variations. We may note that Equation (20), which is valid for $\beta_{\perp C} \to 0$ and $\lambda_C \simeq 0$

predicts a decrease of γ with increasing value of N_H/N_C for a fixed value of $|U_C| = (N_H U_H/N_C)$.

Figure 2 shows that the maximum growth rate γ_m, maximized with respect to λ_C, increases by an increase of core electron drift speed $|U_C|$ (or equivalently halo electron drift U_H) for a fixed value of N_H/N_C (cf. solid curves). The corresponding real frequency, however, shows a slight decrease by an increase in $|U_C|/\alpha_{\perp C}$ (dashed curve 2). The maximum growth rate increases with an increase in $k_\parallel/k_\perp$ (cf. curves 1, 2 and 3) and $T_{\perp C}/T_{\perp H}$ (cf. curves 1 and 4). The dotted portions of the curves 3 and 4, represent the region where the assumption $|\gamma^2| \ll |\omega_r^2|$ breaks down.

Figure 3 shows that γ_m increases by a decrease of $\beta_{\perp C}$ as well as $T_{\parallel H}/T_{\perp H}$ (cf. curves 1, 2, 3, and 4). In the dotted parts of the solid curves, the parameter $|\omega/k_\parallel \alpha_{\parallel C}|$ becomes smaller than 3 and the assumption of $|\omega/k_\parallel \alpha_{\parallel C}|^2 \gg 1$ breaks down.

The variations in the parameters ω_{pC}/Ω_e, $T_{\parallel C}/T_{\perp C}$, $T_{\perp C}/T_p$ are found to affect the maximum growth rate only slightly and, hence, they are not shown here.

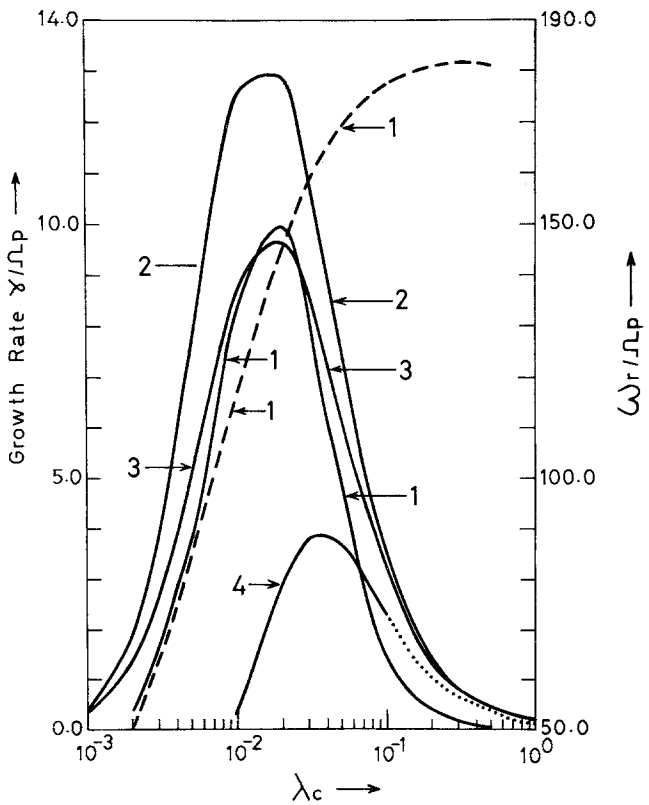

Fig. 1. Variation of growth rate γ/Ω_p (solid curves, ——) and real frequency (dashed curves, – – –) versus λ_C for $\omega_{pC}^2/\Omega_e^2 = 500$, $T_{\perp C}/T_{\perp H} = 0.1$, $T_{\perp H}/T_{\parallel H} = T_{\perp C}/T_{\parallel C} = 1.0$, $T_{\perp C}/T_p = 2.0$, $k_\parallel/k = 0.1$, $\beta_{\perp C} = 0.01$, $U_C/\alpha_{\perp C} = -0.2$, and for $N_H/N_C = 0.001$, 0.01, 0.02, and 0.04 for the curves 1, 2, 3, and 4, respectively. Real frequencies are plotted only for the case of $N_H/N_C = 0.001$ (corresponding to solid curve 1) only.

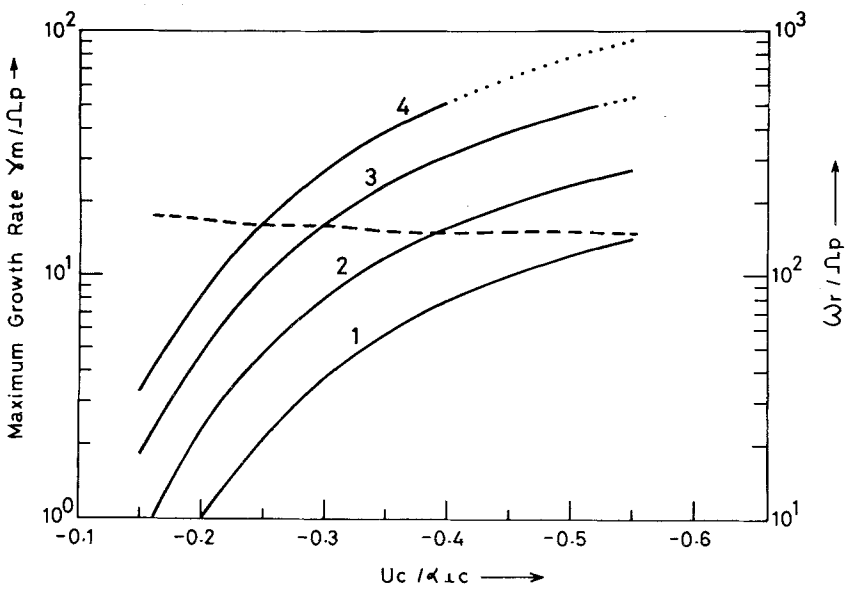

Fig. 2. Variation of maximum growth rates γ_m/Ω_p, maximized with respect to λ_C (solid curves, ——) and corresponding real frequencies (dashed curves – – –) vs core drift speed $U_C/\alpha_{\perp C}$ for the parameters $\omega_{pC}^2/\Omega_e^2 = 500$, $T_{\perp C}/T_p = 2.0$, $N_H/N_C = 0.05$, $\beta_{\perp C} = 0.01$, and for $T_{\perp C}/T_{\perp H} = 0.1$, and $k_\parallel/k = 0.05, 0.01$, and 0.2 for the curves 1, 2, and 3, respectively. The curve 4 is for $k_\parallel/k = 0.1$ and $T_{\perp C}/T_{\perp H} = 0.2$. The real frequencies are shown corresponding to solid curve 2 only.

3. Discussion

The peak growth rates generally occur in the wavenumber regime $0.01 \leq \lambda_C \leq 0.1$ as seen from Figure 1 (this holds true for the parameters of Figures 2 and 3 also). Therefore, the most unstable perpendicular wavelengths associated with the instability are $\lambda_\perp = 2\pi/k_\perp = (60 - 180)\pi\rho_C$ where $\rho_C = (\alpha_{\perp C}/\sqrt{2}\,\Omega_e)$ is the Larmor radius of the core electrons. At 0.3 AU, the most unstable wavelengths would fall in the range from 20 to 90 km, as ρ_C is typically of the order of 150 m there.

In the spacecraft's frame of reference, the frequencies generated by electromagnetic lower hybrid instability would be Doppler-shifted to $\omega_r' = \omega_r \pm \mathbf{k} \cdot \mathbf{V}_{SW}$ where $\mathbf{V}_{SW}$ is the bulk velocity of the solar wind. Assuming $\mathbf{V}_{SW}$ to be along interplanetary magnetic field $\mathbf{B}_0$ and $k_\parallel/k = 0.1$, $\mathbf{V}_{SW} = \alpha_{\perp C}/5$, $\lambda_C = 0.01$–0.1, the Doppler shifts come out to be about $5\Omega_p$ to $15\Omega_p$. The Doppler shifts would, however, be much larger when $\mathbf{V}_{SW}$ is inclined at large angles with respect to $\mathbf{B}_0$. Hence, in general, the noise generated by the instability will be broadband in nature. The bursty nature of the noise at some occasions can be accounted for as arising due to some sudden changes in the plasma parameters like $\beta_{\perp C}$, N_H/N_C, $T_{\perp H}/T_{\parallel H}$, $T_{\perp C}/T_{\perp H}$, etc. Further, such broadband electromagnetic lower hybrid wave noise is expected to give rise to a strong local heating of the ions in the transverse direction and electrons in the parallel direction (Marsch and Chang, 1983; Revathy and Lakhina, 1977).

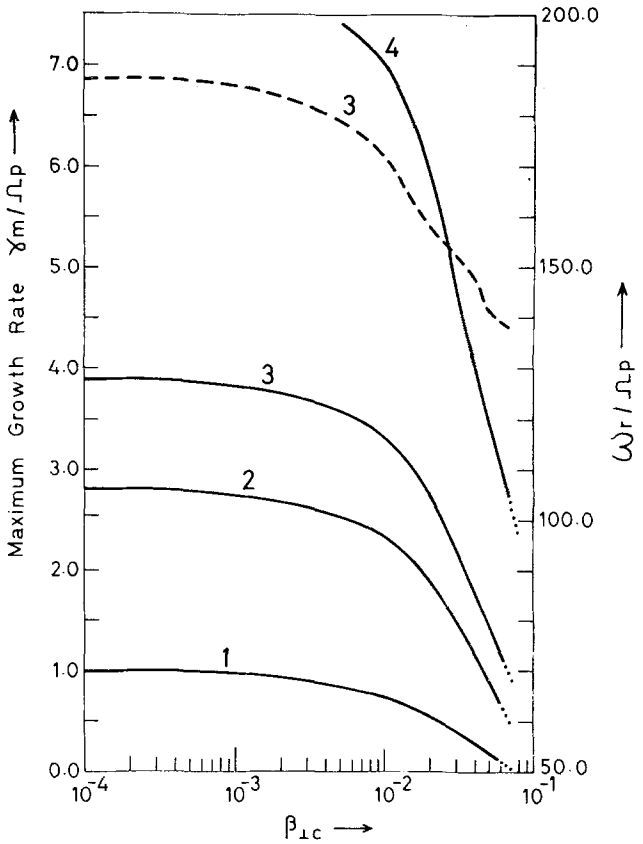

Fig. 3. Variation of γ_m/γ_p (solid curves) and real frequency corresponding to maximum growth rate (dashed curve 3) versus $\beta_{\perp C}$ for $\omega_p^2/\Omega_e^2 = 500.0$, $N_H/N_C = 0.05$, $T_{\parallel C}/T_{\perp C} = 1.0$, $k_\parallel/k = 0.1$, $T_{\perp C}/T_p = 2.0$, and for $T_{\parallel H}/T_{\perp H} = 2.0$, 1.0, 0.8, and 0.5 for the curves 1, 2, 3, and 4, respectively. The dotted portion of the solid curves corresponds to $|\omega/k_\parallel \alpha_{\parallel C}| < 3$, so that assumption $|\omega/k_\parallel \alpha_{\parallel C}|^2 \gg 1$ breaks down in such cases. The curves for real frequencies (dashed curves) follow the scale on the right-hand side of the diagram.

We shall now discuss the B/E ratios or refractive index of the low-frequency noise generated by electromagnetic lower hybrid instability. To a good approximation, the Y-component of the perturbed current density $\mathbf{j}$ can be taken as $j_y \simeq en_0 E_x/B_0$, where E_x is the x-component of the wave electric field. Then from the Maxwell equations, we get for the electromagnetic lower hybrid waves considered here, the relation:

$$\left|\frac{B}{E}\right|^2 = \frac{n^2\left[\frac{k_\parallel^2}{k_\perp^2}(\xi-1)^2 + \frac{\omega_{pe}^4}{\omega^2\Omega_e^2(1-n^2)^2}\right]}{\left[1 + \frac{k_\parallel^2}{k_\perp^2}\xi^2 + \omega_{pe}^4/\Omega_e^2\omega^2(1-n^2)^2\right]}, \tag{21}$$

where $n = (ck/\omega)$ is the refractive index of the wave and $\xi = (E_z k_\perp/k_\parallel E_x)$; E_z being the z-component of wave electric field. The exact numerical value of ξ can be obtained from

the dispersion matrix. For $\xi = 1$, the Maxwell equation $\nabla \times \mathbf{E} = -\partial \mathbf{B}/c\,\partial t$ predicts that $B_y = 0$, and the magnetic field $\mathbf{B}$ of the wave would be predominantly along z-direction. For $\xi > 1$, all the three components of $\mathbf{B}$ would be present. From Equation (21), it is clear that the smallest B/E ratio is obtained for $\xi = 1$.

Coroniti *et al.* (1982) have observed obliquely propagating whistler modes in the frequency range $\Omega_p^2 \ll \omega^2 \ll \Omega_e^2$ in the disturbed solar wind. Coroniti *et al.* (1982) find that these oblique whistler modes have $(B/\eta_\parallel E) = 0.1$–$4.6$, where $\eta_\parallel = (\omega_{pe}^2/\Omega_e\omega)^{1/2}$ is the refractive index of the field-aligned whistler waves ($\mathbf{K} \parallel \mathbf{B}_0$). The waves generated by electromagnetic lower hybrid instability can have such large values of $(B/\eta_\parallel E)$ ratios as shown below. From Figures 1 to 3, we find that maximum growth rate occur around $\omega_{pC}^2/c^2k^2 = \beta_{\perp C}/2\lambda_C \sim \frac{1}{2}$. On taking $\omega_{pc}^2/\Omega_e^2 = 500$ and $\omega_r = 10^2\,\Omega_p$, in Equation (21), we get $(B/\eta_\parallel E) = 0.16$ for $\xi = 1$. However, for $\xi = 4$, Equation (21) yields, $(B/\eta_\parallel E) \simeq 3.6$. Hence, the observed values of $(B/\eta_\parallel E)$ associated with low frequency very oblique whistler modes can be explained in terms of electromagnetic lower hybrid waves provided ξ varies from 1 to 4. In other words, the high values of $(B/\eta_\parallel E)$ are the manifestation of a significant finite $E_z = (\xi k_\parallel E_x/k_\perp)$ component of the wave electric field, which in turn produces large fluctuating B_y component. This shows that the very oblique whistlers observed by Coroniti *et al.* (1982) are indeed the electromagnetic lower hybrid waves as suggested by Marsch and Chang (1983).

The free energy source for the excitation of electromagnetic lower hybrid instability considered here is the electron heat flux carried by the halo electron drift U_H. The beam like feature on the high energy tail of the solar wind electron distribution function would, however, be smeared over a few growth period of the instability. At 0.3 AU, a typical growth period is about $\tau = 25$ ms assuming $\gamma = 10\,\Omega_p$. Hence, a resolved bump-on-tail feature in the electron distribution function may not show up in the data obtained by present day instruments which give a time average resolution of a few seconds.

Our analysis shows that electromagnetic lower hybrid instability is excited when U_H exceeds a threshold value U^*, where $U^* = \omega/k_\parallel$ is simply the parallel phase velocity of the wave. For $(m_e T_{\perp C} k_\perp^2/m_i T_{\perp H} k_\parallel^2) < \beta_{\perp C} \ll 1$, the threshold for onset of the instability, i.e., U^*, can be frequently smaller than $\alpha_{\parallel H}$. For example, for $\beta_{\perp C} = 10^{-2}$, $k_\parallel/k_\perp = 0.1$, Equations (19) and (20), predict $U^* = 0.7\alpha_{\parallel H}$. Numerical computations of γ from Equations (15) and (16) also corroborate this conclusion. However, the growth rate for $U_H \simeq U^*$ are quite small ($\gamma < \Omega_p$); the large growth rates occur for $U_H > \alpha_{\parallel H}$ where U_H significantly exceeds U^* (as seen from Figure 2). Such large halo electron drift (i.e., $U_H > \alpha_{\parallel H}$) can also excite high frequency plasma oscillations with frequencies $\omega \sim \omega_{pC}$. The maximum growth rate, γ_{PW}, of the high frequency plasma waves can be written as (Akhiezer *et al.*, 1975)

$$\gamma_{PW} \simeq \sqrt{\frac{\pi}{8}\,\frac{N_H}{N_C}\,\frac{(U_H - \alpha_{\parallel H})^2}{\alpha_{\parallel H}^2}}\;\omega_{pC}\,. \tag{22}$$

From Equation (22), we note that except for $U_H \approx \alpha_{\parallel H}$ the growth rate for the plasma oscillations would be much higher than those of electromagnetic lower hybrid waves. For example for $U_H \simeq 2\alpha_{\parallel H}$, which corresponds to $|U_C/\alpha_{\perp C}| \simeq 0.32$ in Figure 2,

Equation (22) gives $\gamma_{PW} = 1.4 \times 10^3\ \Omega_p$ whereas the γ_m for electromagnetic lower hybrid instability as seen from Figure 2 is $\gamma_m \lesssim 30\ \Omega_p$. On the other hand for $|U_C/\alpha_{\perp C}| = 0.16$, which gives $U_H = 1.01\alpha_{\| H}$, we have $\gamma_m \simeq 4\ \Omega_p$ (cf. Figure 2) and $\gamma_{PW} = 0.14\ \Omega_p$ (from Equation (22)). Hence, it is clear that when the halo electron drift lies in the range $U^* < U_H \approx \alpha_{\| H}$, the electromagnetic lower hybrid waves would be dominant over the electron plasma wave instability. In fact for $U_H < \alpha_{\| H}$, the latter instability cannot arise in the plasma. This result seems to be in contract to that of Marsch and Chang (1983) who find the simultaneous excitation of electromagnetic lower hybrid waves and the high frequency plasma oscillations for the parametric range considered by them. In reality, there is no contradiction as to start with Marsch and Chang (1983) have considered $U_H/\alpha_{\| H} \simeq 1.9$ (cf. Figures 1 and 2 of their paper) where the high frequency plasma waves are expected to be excited with large growth rates. For the parameters of their Figure 3, the threshold for excitation of electromagnetic lower hybrid instability is around $U_H/\alpha_{\| H} \simeq 2.5$ (as seen from their Figure 3), where, once again, the high frequency plasma waves would have large growth rates as seen by our Equation (22).

In view of above arguments, we suggest that at comparatively low halo electron drifts $U_H > U^* \lesssim \alpha_{\| H}$, the electromagnetic lower hybrid instability would be excited, and it would give rise to the heating of ions and electrons in the transverse and parallel directions, respectively. For $U_H > U^* > \alpha_{\| H}$, both the lower hybrid and high frequency electron plasma waves could exist together, thereby explaining the experimental observations of correlated whistler and plasma oscillation bursts (Kennel *et al.*, 1980).

References

Akhiezer, A. I., Akhiezer, I. A., Polovin, R. V., Sitenko, A. G., and Stepanov, K. N.: 1975, *Plasma Electrodynamics*, Vol. 1, Pergamon Press, New York, p. 291.

Bame, S. J., Asbridge, J. R., Feldman, W. C., Gary, S. P., and Montgomery, M. D.: 1975, *Geophys. Res. Letters* **2**, 373.

Beinroth, H. J. and Neubauer, F. M.: 1981, *J. Geophys. Res.* **86**, 7755.

Coroniti, F. V., Kennel, C. F., Scarf, F. L., Dum, C. T., Marsch, E., Pilipp, W., and Gurnett, D. A.: 1981, in H. Rosenbauer (ed.), *Solar Wind Four*, Rep. MPAE–W–100–81–31, Max-Planck Institut für Aeronomie, Katlenburg-Lindau, F.R.G.

Feldman, W. C., Asbridge, J. R., Bame, S. J., Montgomery, M. D., and Gary, S. P.: 1975, *J. Geophys. Res.* **80**, 4181.

Gurnett, D. A. and Frank, L. A.: 1978, *J. Geophys. Res.* **83**, 58.

Gurnett, D. A., Marsch, E., Pilipp, W., Schwenn, R., and Rosenbauer, H.: 1979, *J. Geophys. Res.* **84**, 2029.

Kennel, C. F., Scarf, F. L., Coroniti, F. V., Fredricks, R. W., Gurnett, D. A., and Smith, E. J.: 1980, *Geophys. Res. Letters* **7**, 129.

Kennel, C. F., Scarf, F. L., and Coroniti, F. V.: 1982, *J. Geophys. Res.* **87**, 17.

Lakhina, G. S.: 1981, in H. Rosenbauer (ed.), *Solar Wind Four*, Rep. MPAE–W–100–81–31, Max-Planck Institut für Aeronomie, Katlenburg-Lindau, F.R.G.

Lakhina, G. S.: 1979, *Astrophys. Space Sci.* **63**, 511.

Marsch, E. and Chang, T.: 1982, *Geophys. Res. Letters* **9**, 1155.

Marsch, E. and Chang, T.: 1983, *J. Geophys. Res.* **88**, 6869.

Marsch, E., Muhlhauser, K. H., Schwenn, R., Rosenbauer, H., Philipp, W., and Neubauer, F.: 1982, *J. Geophys. Res.* **87**, 52.

Revathy, P. and Lakhina, G. S.: 1977, *J. Plasma Phys.* **17**, 133.

Scarf, F. L., Gurnett, D. A., and Kurth, W. S.: 1981, in H. Rosenbauer (ed.), *Solar Wind Four*, MPAE–W–100–81–31, Report Max-Planck Institut für Aeronomie, Katlenburg-Lindau, F.R.G.

Smith, E. J.: 1982, *J. Geophys. Res.* **87**, 6029.